Arnaud RAOUX (arnaud.raoux@sorbonne-universite.fr)
http://www.phys.ens.fr/∼raoux/

Exercise class 8: Quantum Hall Effects

1 Integer quantum Hall effect

In this section, we want to approach a famous phenomenon, that gave rise to several Nobel Prizes: the Quantum Hall Effect.

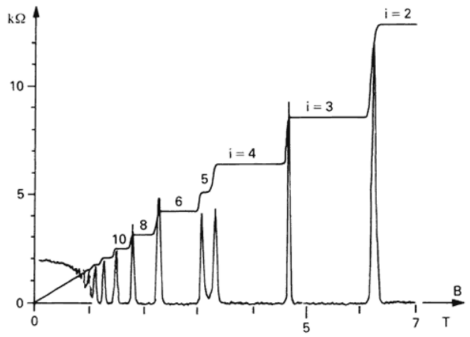

$$\rho_{xy} = \frac{2\pi\hbar}{e^2}\frac{1}{\nu} \qquad \nu \in \mathbf{Z}$$

Figure 1: Resistivity of a 2D sample under a strong magnetic field (and low temperature)

We consider a 2D metallic sample placed inside a perpendicular homogeneous magnetic field B. We will study this problem from the classical and quantum points of view.

1. In a classical approach, describe the trajectory of a charged particle inside such a setup. What happens if one adds an electric field on the sample?

> *Correction.*
> In classical mechanics, the magnetic Lorentz force gives the equation: $m\ddot{\boldsymbol{r}} = -e\dot{\boldsymbol{r}} \times \boldsymbol{B}$. The solutions in the bulk of the system are circular trajectories, which indicates that the system is insulating. On th edges, the electrons can "bounce" on the edge on the sample, and follow skipping orbits that travel on the edges of the sample.
> If we add an electrical current in the x direction, then a voltage in the y direction appears: the classical Hall effect.

2. Using the Heisenberg inequality, propose a typical length ℓ at which quantum effects start to matter for cyclotron orbits.

Correction.
Using the previous question, if the radius of the cyclotron orbit is R, the velocity of the electron is $R\omega_c$ with $\omega_c = \frac{eB}{m}$ the cyclotron pulsation. When $Rmv \sim \hbar$, then the quantum nature of the electron enters in the game. Let ℓ be this radius. Thus: $\ell m\frac{eB}{m}\ell \sim \hbar$, and so:

$$\ell = \sqrt{\frac{\hbar}{eB}} \qquad \text{magnetic length}$$

3. In a quantum mechanical approach, write the Hamiltonian of a charged particle using the operator $\hat{\Pi}_i = \hat{p}_i - qA_i(\hat{\boldsymbol{r}})$.

Correction.

$$\hat{H} = \frac{(\hat{\boldsymbol{P}} - q\boldsymbol{A}(\hat{\boldsymbol{r}}))^2}{2m} = \frac{\hat{\Pi}_x^2}{2m} + \frac{\hat{\Pi}_y^2}{2m}$$

4. Rewrite the Hamiltonian in the form $\hat{H} = \hbar\omega_c(\hat{a}^\dagger\hat{a} + 1/2)$. What is the spectrum associated to this Hamiltonian? We started with two dimensions (x and y), but ended with one quantum number. What can we deduce?

Correction.
To diagonalize $\hat{H}$, we define:

$$\hat{a} = \frac{1}{\sqrt{2\hbar qB}}(\hat{\Pi}_x + i\hat{\Pi}_y) \qquad \text{and} \qquad \hat{a}^\dagger = \frac{1}{\sqrt{2\hbar qB}}(\hat{\Pi}_x - i\hat{\Pi}_y)$$

One can verify that these annihilation and creation operators verify $[\hat{a}, \hat{a}^\dagger] = 1$. Thus the change of operators is "canonical", we can rewrite the Hamiltonian $\hat{H} = \hbar\omega_c(\hat{a}^\dagger\hat{a} + 1/2)$. This is the usual Hamiltonian of an harmonic operator, and the spectrum is thus $E_n = \hbar\omega_c(n + 1/2)$.
Without a magnetic field, all of the possible states can be ordered by the $\boldsymbol{k} = (k_x, k_y)$ vector, with the dispersion relation $E = \frac{\hbar^2}{2m}(k_x^2 + k_y^2)$. But with the magnetic field, we only have one quantum number n. This suggests that each E_n level is highly degenerate.

5. To derive the wave functions, one has to explicitly choose a gauge. In the symmetric gauge $\boldsymbol{A} = \boldsymbol{B} \times \boldsymbol{r}/2$, the eigenfunctions of the lowest Landau level (LLL) reads

$$\psi_m(x, y) = r^m \, \mathrm{e}^{im\varphi} \, \mathrm{e}^{-r^2/4\ell^2} \tag{1}$$

What is the typical size of the radial probability density $r|\psi_m|^2$ as a function of m?

Correction.
The maximum of the radial probability is given by a vanishing derivative:

$$\frac{\mathrm{d}}{\mathrm{d}r}(r|\psi|^2) = \frac{\mathrm{d}}{\mathrm{d}r}\left(r^{2m+1}\,\mathrm{e}^{-r^2/2\ell^2}\right) = \left[(2m+1)r^{2m} - \frac{r^{2m+2}}{\ell^2}\right]\mathrm{e}^{-r^2/2\ell^2} = 0$$

Thus the radius at which the radial probability of ψ_m is maximum is $r_m = \ell\sqrt{2(m+1)}$.

6. If the sample has a surface S, calculate the degeneracy $\mathcal{D}$ of the LLL. Give an expression of $\mathcal{D}$ in terms of $\Phi_0 = h/q$ the flux quantum, and $\Phi = BS$ the magnetic flux inside the sample.

Correction.
Let's calculate the surface s_m that is occupied by a state ψ_m:

$$\begin{aligned} s_m = 2\pi r_m(r_{m+1} - r_m) &= 2\pi\ell^2\sqrt{2(m+1)}(\sqrt{2(m+2)} - \sqrt{2(m+1)}) \\ &= 4\pi\ell^2(m+1)(\sqrt{\frac{m+2}{m+1}} - 1) \\ &\approx 2\pi\ell^2 \end{aligned}$$

At first order, s_m is independent of m. We deduce the degeneracy of the LLL by simply calculating S/s_m:

$$\mathcal{D} = \frac{S}{s_m} = \frac{eBS}{2\pi\hbar} = \frac{\Phi}{\Phi_0}$$

For a typical system in high magnetic field $BS \sim 1\,\mathrm{mm}^2 \times 7\,\mathrm{T} = 7 \times 10^{-6}\,\mathrm{Wb}$. The flux quantum is $h/e = 4 \times 10^{-15}\,\mathrm{Wb}$, so there is indeed a macroscopic degeneracy of the LLL. One can show that all of the LL are macroscopically degenerate.

7. Now, we fill the levels with fermions, up to the Fermi energy μ. Describe the conducting state of the sample depending on the value of μ.

Correction.
There are two possibilities:

- If the chemical potential is at the energy of a LL, then this LL is partially filled, and there are a huge number of states that can serve the electrical conduction. The conductivity is high.
- If the chemical potential lies in between two LLs, then there are no states available to excite electrons and get a electrical current. The system is insulating.

This is an extreme situation. But taking into account temperature and disorder will render this picture smoother by giving a typical width to LL. If the typical length is smaller than the distance between LL (high magnetic field situation), then the situation is basically the same as described above but a little smoother. If the spread of the LL is bigger that the spacing between LLs (small field situation), then the discrete nature of LLs disappears, and we recover a usual (bad) metallic system.
Note: In a high magnetic field environment, there is a counter-intuitive fact. Because resistivity and conductivity are now 2×2 matrices, $\rho = \sigma^{-1}$ is still true, but $\rho_{xx} \neq \sigma_{xx}^{-1}$. Indeed, a simple matrix inversion gives $\sigma_{xx} = \frac{\rho_{xx}}{\rho_{xx}^2+\rho_{xy}^2}$. In the case where ρ_{xy} is high, one can see that ρ_{xx} is actually **proportional** to σ_{xx}.

8. The edges of the sample act as a repulsive potential. Suggest a modification of the Landau levels structure taking into account those edges. Suppose now that the chemical potential lies between two LLs. Explain why the sample is insulating in the bulk, but conductive on the edges.

Correction.
The LLs are flat in the bulk, but because the boundaries of the sample act as a repulsive potential, the LLs are deformed near the edges of the system. Thus, what ever the position of the chemical potential, it crosses some edge states. More accurately, if there are n filled LLs below the chemical potential, then it crosses n edge states that are all going in the same direction. All the states are *chiral* (go in the same direction), this direction depends on the magnetic field.

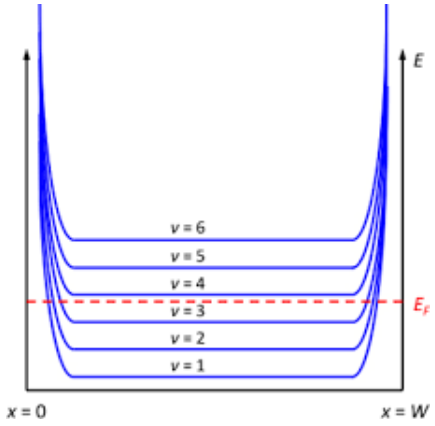

2 Quantum Spin Hall Effect

The Quantum Spin Hall Effect has been theoretically proposed by Kane & Mele in 2005 in two articles: one which gives a possible realization in Graphene [1] and another one that describes precisely the topological implications [2]. A year later, a proposal to measure the QSHE in HgTe Quantum wells was published [3], and actually discovered a year later [4].

For this session, we focus on the article on Graphene, and the theoretical realization of the QSHE. The article is attached: *read in priority the three first pages.*

2.1 Hamiltonian in presence of spin-orbit coupling

9. Using a previous exercise session, write the approximate Hamiltonian for a spinless electron near a K point, then deduce the Fourier transform expression in the real space. What will be the Hamiltonian near a $\tilde{K}$ point?

Correction.
We have shown in the homework that near a Dirac point, the linearized Hamiltonian is given by

$$H_K = \hbar v_F \begin{pmatrix} 0 & q^\star \\ q & 0 \end{pmatrix} = \hbar v_F (q_x \sigma_x + q_y \sigma_y) \tag{2}$$

If we want the come back to real space, then we should replace $iq_x \to \partial_x$ and $iq_y \to \partial_y$.
In the $\tilde{K}$ point, we get the complex conjugate of H_K.

10. Explain the expression in Eq. (2) and find the associated energy spectrum.

Correction.
In Eq. (2) there are two sets of Pauli matrices: σ_i for the sublattice and τ_i for the choice of the valley. Indeed, at a given energy near 0, the available states are either near a K point, or near a $\tilde{K}$ point. Thus, the total Hamiltonian for a spinless electron is:

$$H_k = \begin{pmatrix} H_K & 0 \\ 0 & H_{\tilde{K}} \end{pmatrix} = \hbar v_F \begin{pmatrix} \begin{pmatrix} 0 & q^\star \\ q & 0 \end{pmatrix} & 0 \\ 0 & \begin{pmatrix} 0 & q \\ q^\star & 0 \end{pmatrix} \end{pmatrix}$$

H_K and $H_{\tilde{K}}$ have the same spectrum, so the spectrum of H_k is twice degenerate, with $E = \pm\hbar v_F |q|$.

11. What does the addition of a σ_z or $\sigma_z\tau_z$ term in the Hamiltonian? Can you give a symmetry explanation?

Correction.
Adding a term proportional to σ_z breaks the chiral symmetry of the system, and $\sigma_z\tau_z$ breaks the TRS. Thus the degeneracies in K points are not topologically protected anymore and a gap opens.

12. Explain the sentence: *The gap parameter $\sigma_z\tau_z s_z$ produces gaps with opposite signs at the K and K' points*

Correction.
Adding such a term will indeed open a gap as the calculation of the spectrum will show. The "sign" of the gap is a shortcut that means that the d_z component of the $\boldsymbol{d}$ vector representing the Hamiltonian on the Bloch sphere will change sign between K and $\tilde{K}$. Thus, $\boldsymbol{d}$ will wrap around the sphere at least once which creates a non-trivial topological structure.

2.2 Edge states

13. Justify what is topological in this problem. Can you guess the possible values of the topological invariant?

Correction.
The edge states are topologically protected, so because of the bulk-edge correspondance, there should be some bulk topological quantity. Not that because TRS is preserved, this invariant can not be the Chern number.
We know at least two distinct phases: one with no edge states, and one with two edge states (what we call a Kramers pair). What about 4 edge states? Now the four edge states can scatter one from another, and the degeneracy will be lifted. A gap will open, and we come back to the situation without any edge states. Finally, we understand that there only exist two topologically different phases. We have a $\mathbb{Z}_2$ invariant.

14. Focus on Fig. (2): explain the experimental expectations of the QSHE, and compare it to the IQHE.

Correction.

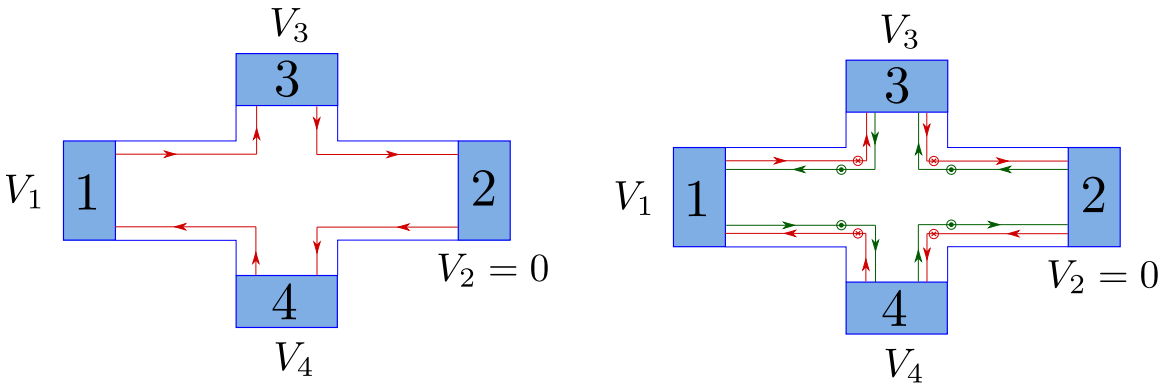

Let us first consider the case of the IQHE with the geometry of the left figure. We impose a electrical current through terminals 1 and 2. Let's suppose for the sake of the argument that the chiral edge states move in a clockwise direction. Landauer-Büttiker formalism is needed to understand in details what is happening, but let's try to give a qualitative picture. Electrodes 1 and 2 are electrons reservoirs, and they will impose their chemical potential to other electrodes if they are lined by some conducting channels. Because of the chirality of the edge states, electrode 1 only influence electrode 3 and $V_1 = V_3$. Similarly $V_2 = V_4 = 0$. Thus because of the electrical current, there exist a transverse Hall voltage $V_3 - V_4$.
Let's now move on the QSHE on the right side, and let's suppose that there is a voltage between 1 and 2. Because electrodes 3 and 4 are both linked to electrodes 1 and 2, electrodes 3 and 4 and electrically symmetrical, so $V_3 = V_4$. However, they are not furnished with electrons with the same spin. In this configuration $V_1 > V_2 = 0$, more electrons leave electrode 2 than electrode 1. So electrode 3 will be furnished essentially with spin down electrons, and electrode 4 with spin up. There is thus a *spin current* between electrodes 3 and 4.

References

[1] Kane & Mele., "Quantum Spin Hall Effect in Graphene", Phys. Rev. Lett. **95**, 226801 (2005).

[2] Kane & Mele., "Z_2 Topological Oder ad the Quantum Spin Hall Effect", Phys. Rev. Lett. **95**, 146802 (2005).

[3] Bernevig, Hugues & Zhang, "Quantum Spin Hall Effect and Topological Phase Transition in HgTe Quantum Wells", Science **314**, 5806 (2006).

[4] König et al., "Quantum Spin Hall Insulator State in HgTe Quantum Wells", Science **318**, 5851 (2007).

Quantum Spin Hall Effect in Graphene

C. L. Kane and E. J. Mele

Dept. of Physics and Astronomy, University of Pennsylvania, Philadelphia, Pennsylvania 19104, USA

(Received 29 November 2004; published 23 November 2005)

We study the effects of spin orbit interactions on the low energy electronic structure of a single plane of graphene. We find that in an experimentally accessible low temperature regime the symmetry allowed spin orbit potential converts graphene from an ideal two-dimensional semimetallic state to a quantum spin Hall insulator. This novel electronic state of matter is gapped in the bulk and supports the transport of spin and charge in gapless edge states that propagate at the sample boundaries. The edge states are nonchiral, but they are insensitive to disorder because their directionality is correlated with spin. The spin and charge conductances in these edge states are calculated and the effects of temperature, chemical potential, Rashba coupling, disorder, and symmetry breaking fields are discussed.

DOI: 10.1103/PhysRevLett.95.226801 PACS numbers: 73.43.−f, 72.25.Hg, 73.61.Wp, 85.75.−d

The generation of spin current solid state systems has been a focus of intense recent interest. It has been argued that in doped semiconductors the spin orbit (SO) interaction leads to a spin Hall effect [1,2], in which a spin current flows perpendicular to an applied electric field. The spin Hall effect has been observed in GaAs [3,4]. Murakami *et al.* [5] have identified a class of cubic materials that are insulators, but nonetheless exhibit a finite spin Hall conductivity. Such a ''spin Hall insulator'' would be of intrinsic interest, since it would allow for spin currents to be generated without dissipation.

In this Letter we show that at sufficiently low energy a single plane of graphene exhibits a quantum spin Hall (QSH) effect with an energy gap that is generated by the SO interaction. Our motivation is twofold. First, Novoselov *et al.* [6] have recently reported progress in the preparation of single layer graphene films. These films exhibit the expected ambipolar behavior when gated and have mobilities up to $10^4 \mathrm{cm}^2/\mathrm{V\,s}$. Thus, the detailed experimental study of graphene now appears feasible. We believe the QSH effect in graphene is observable below a low but experimentally accessible temperature. Secondly, we will show the QSH effect in graphene is different from the spin Hall effects studied for three-dimensional cubic systems in Ref. [5] because it leads to a phase which is *topologically distinct* from a band insulator. The QSH effect in graphene resembles the charge quantum Hall effect, and we will show that spin and charge currents can be transported in gapless edge states. As a model system, graphene thus identifies a new class of spin Hall insulator. It may provide a starting point for the search for other spin Hall insulators in two-dimensional or in layered materials with stronger SO interaction.

SO effects in graphite have been known for over 40 years [7], and play a role in the formation of minority hole pockets in the graphite Fermi surface [8]. However, these effects have largely been ignored because they are predicted to be quite small and they are overwhelmed by the larger effect of coupling between the graphene planes. Unlike graphite which has a finite Fermi surface, however, graphene is in a critical electronic state which can be strongly affected by small perturbations at low energy.

Graphene consists of a honeycomb lattice of carbon atoms with two sublattices. The states near the Fermi energy are π orbitals residing near the K and K' points at opposite corners of the hexagonal Brillouin zone. An effective mass model can be developed [9] by writing the low energy electronic wavefunctions as

$$\Psi(\mathbf{r}) = [(u_{AK}, u_{BK}), (u_{AK'}, u_{BK'})]\psi(\mathbf{r}) \tag{1}$$

where $u_{(A,B)(K,K')}(\mathbf{r})$ describe basis states at momentum $k = K, K'$ centered on atoms of the A, B sublattice. $\psi(\mathbf{r})$ is a four component slowly varying envelope function. The effective mass Hamiltonian then takes the form,

$$\mathcal{H}_0 = -i\hbar v_F \psi^\dagger(\sigma_x\tau_z\partial_x + \sigma_y\partial_y)\psi. \tag{2}$$

Here $\vec{\sigma}$ and $\vec{\tau}$ are Pauli matrices with $\sigma_z = \pm 1$ describing states on the $A(B)$ sublattice and $\tau_z = \pm 1$ describing states at the $K(K')$ points. This Hamiltonian describes gapless states with $E(\mathbf{q}) = \pm v_F|\mathbf{q}|$. Without spin, the degeneracy at $\mathbf{q} = 0$ is protected by symmetry. The only possible terms that could be added to open a gap are proportional to σ_z or $\sigma_z\tau_z$. The σ_z term, which corresponds to a staggered sublattice potential is odd under parity (which interchanges the A and B sublattices). The $\sigma_z\tau_z$ term is even under parity, but odd under time reversal (which interchanges K and K').

The SO interaction allows for a new term, which will be the focus of this Letter:

$$\mathcal{H}_{\mathrm{SO}} = \Delta_{so}\psi^\dagger\sigma_z\tau_z s_z\psi. \tag{3}$$

Here s_z is a Pauli matrix representing the electron's spin. This term respects all of the symmetries of graphene, and will be present. Below we will explicitly construct this term from the microscopic SO interaction and estimate its magnitude. If the mirror symmetry about the plane is

preserved then this is the only allowed spin dependent term at $\mathbf{q} = 0$. If the mirror symmetry is broken (either by a perpendicular electric field or by interaction with a substrate) then a Rashba term [10] of the form $(\mathbf{s} \times \mathbf{p}) \cdot \hat{z}$ is allowed,

$$\mathcal{H}_R = \lambda_R \psi^\dagger (\sigma_x \tau_z s_y - \sigma_y s_x) \psi. \quad (4)$$

For $\lambda_R = 0$, Δ_{so} leads to an energy gap $2\Delta_{so}$ with $E(\mathbf{q}) = \pm\sqrt{(\hbar v_F q)^2 + \Delta_{so}^2}$. For $0 < \lambda_R < \Delta_{so}$ the energy gap $2(\Delta_{so} - \lambda_R)$ remains finite. For $\lambda_R > \Delta_{so}$ the gap closes, and the electronic structure is that of a zero gap semiconductor with quadradically dispersing bands. In the following we will assume that $\lambda_R < \Delta_{so}$ and analyze the properties of the resulting gapped phase. This assumption is justified by numerical estimates given at the end of the Letter.

The gap generated by $\sigma_z \tau_z s_z$ is different from the gap that would be generated by the staggered sublattice potentials, σ_z or $\sigma_z s_z$. The ground states in the presence of the latter terms are adiabatically connected to simple insulating phases at strong coupling where the two sublattices are decoupled. In contrast, the gap parameter $\sigma_z \tau_z s_z$ produces gaps with *opposite signs* at the K and K' points. This has no simple strong coupling limit. To connect smoothly between the states generated by σ_z and $\sigma_z \tau_z s_z$ one must pass through a critical point where the gap vanishes, separating ground states with distinct topological orders.

The interaction (3) is related to a model introduced by Haldane [11] as a realization of the parity anomaly in (2 + 1)-dimensional relativistic field theory. Taken separately, the Hamiltonians for the $s_z = \pm 1$ spins violate time reversal symmetry and are equivalent to Haldane's model for spinless electrons, which could be realized by introducing a periodic magnetic field with no net flux. As Haldane showed, this gives rise to a $\sigma_z \tau_z$ gap, which has opposite signs at the K and K' points. At temperatures well below the energy gap this leads to a quantized Hall conductance $\sigma_{xy} = \pm e^2/h$. This Hall conductance computed by the Kubo formula can be interpreted as the topological Chern number induced by the Berry's curvature in momentum space [12,13]. Since the signs of the gaps in (3) are opposite for opposite spins, an electric field will induce opposite currents for the opposite spins, leading to a spin current $\mathbf{J}_s = (\hbar/2e)(\mathbf{J}_\uparrow - \mathbf{J}_\downarrow)$ characterized by a quantized spin Hall conductivity

$$\sigma_{xy}^s = \frac{e}{2\pi}. \quad (5)$$

Since spin currents do not couple to experimental probes it is difficult to directly measure (5). Moreover, the conservation of s_z will be violated by the Rashba term (4) as well as terms which couple the π and σ orbitals. Nonetheless, Murakami *et al.* [14] have defined a conserved spin $s_{z(c)}$, allowing σ_{xy}^s to be computed via the Kubo formula. We find that σ_{xy}^s computed in this way is not quantized when $\lambda_R \neq 0$, though the correction to (5) is small due to carbon's weak SO interaction.

In the quantum Hall effect the bulk topological order requires the presence of gapless edge states. We now show that gapless edge states are also present in graphene. We will begin by establishing the edge states for $\lambda_R = 0$. We will then argue that the gapless edge states persist even when $\lambda_R \neq 0$, and that they are robust against weak electron-electron interactions and disorder. Thus, in spite of the violation of (5) the gapless edge states characterize a state which is distinct from an ordinary insulator. This QSH state is different from the insulators discussed in Ref. [5], which do not have edge states. It is also distinct from the spin Hall effect in doped GaAs, which does not have an energy gap.

For $\lambda_R = 0$, the Hamiltonian (2) and (3) conserves s_z, and the gapless edge states follow from Laughlin's argument [15]. Consider a large cylinder (larger than $\hbar v_F/\Delta_{so}$) and adiabatically insert a quantum $\phi = h/e$ of magnetic flux quantum down the cylinder (slower than $\Delta_{so}/\hbar$). The resulting azimuthal Faraday electric field induces a spin current such that spin $\hbar$ is transported from one end of the cylinder to the other. Since an adiabatic change in the magnetic field cannot excite a particle across the energy gap Δ_{so} it follows that there must be gapless states at each end to accommodate the extra spin.

An explicit description of the edge states requires a model that gives the energy bands throughout the entire Brillouin zone. Following Haldane [11], we introduce a second neighbor tight binding model,

$$\mathcal{H} = \sum_{\langle ij \rangle \alpha} t c_{i\alpha}^\dagger c_{j\alpha} + \sum_{\langle\langle ij \rangle\rangle \alpha\beta} i t_2 \nu_{ij} s_{\alpha\beta}^z c_{i\alpha}^\dagger c_{j\beta}. \quad (6)$$

The first term is the usual nearest neighbor hopping term. The second term connects second neighbors with a spin dependent amplitude. $\nu_{ij} = -\nu_{ji} = \pm 1$, depending on the orientation of the two nearest neighbor bonds $\mathbf{d}_1$ and $\mathbf{d}_2$ the electron traverses in going from site j to i. $\nu_{ij} = +1\,(-1)$ if the electron makes a left (right) turn to get to the second bond. The spin dependent term can be written in a coordinate independent representation as $i(\mathbf{d}_1 \times \mathbf{d}_2) \cdot \mathbf{s}$. At low energy (6) reduces to (2) and (3) with $\Delta_{so} = 3\sqrt{3} t_2$.

The edge states can be seen by solving (7) in a strip geometry. Figure 1 shows the one-dimensional energy bands for a strip where the edges are along the zigzag direction in the graphene plane. The bulk band gaps at the one-dimensional projections of the K and K' points are clearly seen. In addition two bands traverse the gap, connecting the K and K' points. These bands are localized at the edges of the strip, and each band has degenerate copies for each edge. The edge states are not chiral since each edge has states which propagate in both directions. However, as illustrated in Fig. 2 the edge states are "spin filtered" in the sense that electrons with opposite spin propagate in *opposite* directions. Similar edge states occur for armchair edges, though in that case the 1D projections

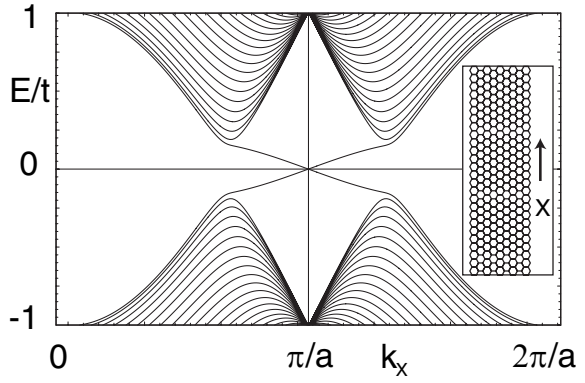

FIG. 1. (a) One-dimensional energy bands for a strip of graphene (shown in inset) modeled by (7) with $t_2/t = 0.03$. The bands crossing the gap are spin filtered edge states.

of K and K' are both at $k = 0$. It is interesting to note that for zigzag edges the edge states persist for $\Delta_{so} \to 0$, where they become perfectly flat [16]. This leads to an enhanced density of states at the Fermi energy associated with zigzag edges. This has been recently seen in scanning tunneling spectroscopy of graphite surfaces [17].

We have also considered a nearest neighbor Rashba term, of the form $i\hat{z} \cdot (\mathbf{s}_{\alpha\beta} \times \mathbf{d}) c^\dagger_{i\alpha} c_{j\beta}$. This violates the conservation of s_z, so that the Laughlin argument no longer applies. Nonetheless, we find that the gapless edge states remain, provided $\lambda_R < \Delta_{so}$, so that the bulk band gap remains intact. The crossing of the edge states at the Brillouin zone boundary $k_x = \pi/a$ in Fig. 1 (or at $k = 0$ for the armchair edge) is protected by time reversal symmetry. The two states at $k_x = \pi/a$ form a Kramers doublet whose degeneracy cannot be lifted by any time reversal symmetric perturbation. Moreover, the degenerate states at $k_x = \pi/a \pm q$ are a Kramers doublet. This means that elastic backscattering from a random potential is forbidden. More generally, scattering from a region of disorder can be characterized by a 2×2 unitary S matrix which relates the incoming and outgoing states: $\Phi_{out} = S\Phi_{in}$, where Φ is a two component spinor consisting of the left and right moving edge states $\phi_{L\uparrow}$, $\phi_{R\downarrow}$. Under time reversal $\Phi_{in,out} \to s_y \Phi^*_{out,in}$. Time reversal symmetry therefore imposes the constraint $S = s_y S^T s_y$, which rules out any off diagonal elements.

Electron interactions can lead to backscattering. For instance, the term $u\psi^\dagger_{L\uparrow}\partial_x\psi^\dagger_{L\uparrow}\psi_{R\downarrow}\partial_x\psi_{R\downarrow}$, does not violate time reversal, and will be present in an interacting Hamiltonian. For weak interactions this term is *irrelevant* under the renormalization group, since its scaling dimension is $\Delta = 4$. It thus will not lead to an energy gap or to localization. Nonetheless, it allows inelastic backscattering. To leading order in u it gives a finite *conductivity* of the edge states, which diverges at low temperature as $u^{-2}T^{3-2\Delta}$ [18]. Since elastic backscattering is prevented by time reversal there are no relevant backscattering processes for weak interactions. This stability against interactions and disorder distinguishes the spin filtered edge states from ordinary one-dimensional wires, which are localized by weak disorder.

A parallel magnetic field $H_\parallel$ breaks time reversal and leads to an avoided crossing of the edge states. $H_\parallel$ also reduces the symmetry, allowing terms in the Hamiltonian which provide a continuously gapped path connecting the states generated by $\sigma_z\tau_z s_z$ and σ_z. Thus in addition to gapping the edge states $H_\parallel$ eliminates the topological distinction between the QSH phase and a simple insulator.

The spin filtered edge states have important consequences for both the transport of charge and spin. In the limit of low temperature we may ignore the inelastic backscattering processes, and describe the ballistic transport in the edge states within a Landauer-Büttiker [19] framework. For a two terminal geometry [Fig. 2(a)], we predict a ballistic two terminal charge conductance $G = 2e^2/h$. For the spin filtered edge states the edge current density is related to the spin density, since both depend on $n_{R\uparrow} - n_{L\downarrow}$. Thus the charge current is accompanied by spin accumulation at the edges. The interplay between charge and spin can be probed in a multiterminal device. Define the multiterminal spin conductance by $I^s_i = \sum_j G^s_{ij} V_j$. Time reversal symmetry requires $G^s_{ji} = -G^s_{ij}$, and from Fig. 2(b) it is clear that $G^s_{ij} = \pm e/4\pi$ for adjacent contacts i and j. In the four terminal geometry of Fig. 2(b) a spin current $I^s = eV/4\pi$ flows into the right contact. This geometry can also be used to *measure* a spin current. A spin current incident from the left (injected, for instance,

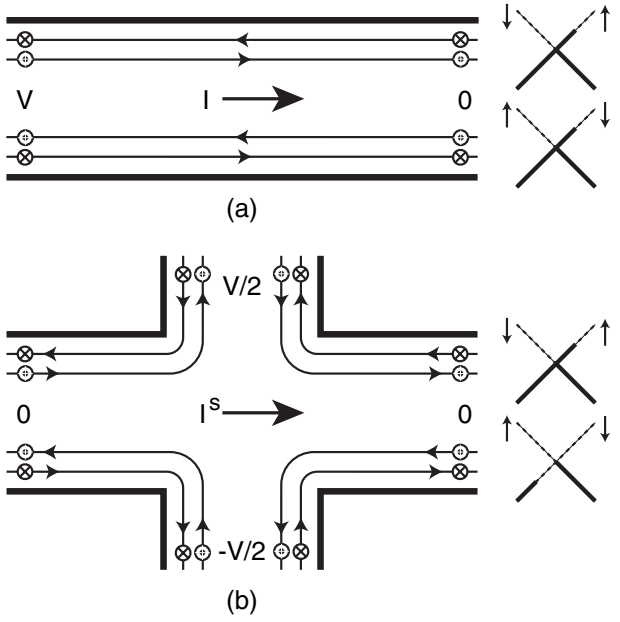

FIG. 2. Schematic diagrams showing (a) two terminal and (b) four terminal measurement geometries. In (a) a charge current $I = (2e^2/h)$ V flows into the right lead. In (b) a spin current $I^s = (e/4\pi)$ V flows into the right lead. The diagrams to the right indicate the population of the edge states.

with a ferromagnetic contact) will be split, with the up (down) spins transported to the top (bottom) contacts, generating a measurable spin Hall voltage.

The magnitude of $\Delta_{\rm so}$ may be estimated by treating the microsopic SO interaction

$$V_{\rm SO} = \frac{\hbar}{4m^2c^2}\mathbf{s}\cdot(\nabla V \times \mathbf{p}) \tag{7}$$

in first order degenerate perturbation theory. We thus evaluate the expectation value of (8) in the basis of states given in (1) treating $\psi(\mathbf{r})$ as a constant. A full evaluation depends on the detailed form of the Bloch functions. However a simple estimate can be made in the "first star" approximation: $u_{(K,K'),(A,B)}(\mathbf{r}) = \sum_p \exp[i\mathbf{K}_p\cdot(\mathbf{r}-\mathbf{d})]/\sqrt{3}$. Here $\mathbf{K}_p$ are the crystal momenta at the three corners of the Brillouin zone equivalent to K or K', and $\mathbf{d}$ is the a basis vector from a hexagon center to an A or B sublattice site. We find that the matrix elements have precisely the structure (3), and using the Coulomb interaction $V(r) = e^2/r$ we estimate $2\Delta_{\rm so} = 4\pi^2e^2\hbar^2/(3m^2c^2a^3) \sim 2.4\,\mathrm{K}$. This is a crude estimate, but it is comparable to the SO splittings quoted in the graphite literature [8].

The Rashba interaction due to a perpendicular electric field E_z may be estimated as $\lambda_R = \hbar v_F e E_z/(4mc^2)$. For $E_z \sim 50$ V/300 nm [3] this gives $\lambda_R \sim 0.5$ mK. This is smaller than $\Delta_{\rm so}$ because E_z is weaker than the atomic scale field. The Rashba term due to interaction with a substrate is more difficult to estimate, though since it is presumably a weak Van der Waals interaction, this too can be expected to be smaller than $\Delta_{\rm so}$.

This estimate of $\Delta_{\rm so}$ ignores the effect of electron-electron interactions. The long range Coulomb interaction may substantially increase the energy gap. To leading order the SO potential is renormalized by the diagram shown in Fig. 3, which physically represents the interaction of electrons with the exchange potential induced by $\Delta_{\rm so}$. This is similar in spirit to the gap renormalizations in 1D Luttinger liquids and leads to a logarithmically divergent correction to $\Delta_{\rm so}$. The divergence is due to the long range $1/r$ Coulomb interaction, which persists in graphene even accounting for screening [20]. The divergent corrections to $\Delta_{\rm so}$ as well as similar corrections to $\hbar v_F$ can be summed using the renormalization group (RG) [20]. Introducing the dimensionless Coulomb interaction $g = e^2/\hbar v_F$ we integrate out the high energy degrees of freedom with energy between Λ and $\Lambda e^{-\ell}$. To leading order in g the RG flow equations are

$$dg/d\ell = -g^2/4; \qquad d\Delta_{\rm so}/d\ell = g\Delta_{\rm so}/2. \tag{8}$$

These equations can be integrated, and at energy scale ε, $\Delta_{\rm so}(\varepsilon) = \Delta^0_{\rm so}[1 + (g^0/4)\log(\Lambda^0/\varepsilon)]^2$. Here g^0 and $\Delta^0_{\rm so}$ are the interactions at cutoff scale Λ^0. The renormalized gap is determined by $\Delta^R_{\rm so} \sim \Delta_{\rm so}(\Delta^R_{\rm so})$. Using an effective interaction $g^0 = 0.74$ [21] and $\Lambda^0 \sim 2$ eV this leads to $2\Delta^R_{\rm so} \sim 15$ K.

FIG. 3. Feynman diagram describing the renormalization of the SO potential by the Coulomb interaction. The solid line represents the electron propagator and the wavy line is the Coulomb interaction.

In summary, we have shown that the ground state of a single plane of graphene exhibits a QSH effect, and has a nontrivial topological order that is robust against small perturbations. The QSH phase should be observable by studying low temperature charge transport and spin injection in samples of graphene with sufficient size and purity to allow the bulk energy gap to manifest itself. It would also be of interest to find other materials with stronger SO coupling which exhibit this effect, as well as possible three-dimensional generalizations.

We thank J. Kikkawa and S. Murakami for helpful discussions. This work was supported by the NSF under MRSEC Grant No. DMR-00-79909 and the DOE under Grant No. DE-FG02-ER-0145118.

[1] S. Murakami, N. Nagaosa, and S. C. Zhang, Science **301**, 1348 (2003).
[2] J. Sinova *et al.*, Phys. Rev. Lett. **92**, 126603 (2004).
[3] Y. K. Kato *et al.*, Science **306**, 1910 (2004).
[4] J. Wunderlich *et al.*, Phys. Rev. Lett. **94**, 047204 (2005).
[5] S. Murakami, N. Nagaosa, and S. C. Zhang, Phys. Rev. Lett. **93**, 156804 (2004).
[6] K. S. Novoselov *et al.*, Science **306**, 666 (2004).
[7] G. Dresselhaus and M. S. Dresselhaus, Phys. Rev. **140**, A401 (1965).
[8] N. B. Brandt, S. M. Chudinov, and Y. G. Ponomarav, *Semimetals 1. Graphite and its Compounds* (North Holland, Amsterdam, 1988).
[9] D. P. DiVincenzo and E. J. Mele, Phys. Rev. B **29**, 1685 (1984).
[10] Y. A. Bychkov and E. I. Rashba, J. Phys. C **17**, 6039 (1984).
[11] F. D. M. Haldane, Phys. Rev. Lett. **61**, 2015 (1988).
[12] D. J. Thouless, M. Kohmoto, M. P. Nightingale, and M. den Nijs, Phys. Rev. Lett. **49**, 405 (1982).
[13] F. D. M. Haldane, Phys. Rev. Lett. **93**, 206602 (2004).
[14] S. Murakami, N. Nagaosa, and S. C. Zhang, Phys. Rev. B **69**, 235206 (2004).
[15] R. B. Laughlin, Phys. Rev. B **23**, R5632 (1981).
[16] M. Fujita *et al.* J. Phys. Soc. Jpn. **65**, 1920 (1996).
[17] Y. Niimi *et al.*, Phys. Rev. B **70**, 214430 (2004).
[18] T. Giamarchi and H. Schulz, Phys. Rev. B **37**, 325 (1988).
[19] M. Büttiker, Phys. Rev. B **38**, 9375 (1988).
[20] J. Gonzalez, F. Guinea, and M. A. H. Vozmediano, Phys. Rev. B **59**, R2474 (1999).
[21] C. L. Kane and E. J. Mele, Phys. Rev. Lett. **93**, 197402 (2004).